

## WATER-PLANETS IN THE HABITABLE ZONE: ATMOSPHERIC CHEMISTRY, OBSERVABLE FEATURES, AND THE CASE OF KEPLER-62*e* AND -62*f*

L. KALTENEGGER<sup>1,2</sup>, D. SASSELOV<sup>2</sup>, AND S. RUGHEIMER<sup>2</sup>

<sup>1</sup> Max Planck Institute of Astronomy, Königstuhl 17, D-69115 Heidelberg, Germany; [kaltenegger@mpia.de](mailto:kaltenegger@mpia.de)

<sup>2</sup> Harvard-Smithsonian Center for Astrophysics, Cambridge, MA 02138, USA

Received 2013 April 2; accepted 2013 August 19; published 2013 September 18

### ABSTRACT

Planets composed of large quantities of water that reside in the habitable zone are expected to have distinct geophysics and geochemistry of their surfaces and atmospheres. We explore these properties motivated by two key questions: whether such planets could provide habitable conditions and whether they exhibit discernable spectral features that distinguish a water-planet from a rocky Earth-like planet. We show that the recently discovered planets Kepler-62*e* and -62*f* are the first viable candidates for habitable zone water-planets. We use these planets as test cases for discussing those differences in detail. We generate atmospheric spectral models and find that potentially habitable water-planets show a distinctive spectral fingerprint in transit depending on their position in the habitable zone.

*Key words:* astrobiology – planets and satellites: atmospheres – planets and satellites: detection – planets and satellites: individual (Kepler-62*f*, Kepler-62*e*, Kepler-69*c*)

*Online-only material:* color figures

### 1. INTRODUCTION

The possible existence of Earth- and super-Earth size<sup>3</sup> planets completely covered by a water envelope has long fascinated scientists and the general public alike (Kuchner 2003; Leger et al. 2004; Selsis et al. 2007). No such planets are known in the solar system but small bodies like Pluto are composed of substantial quantities of water though none are in the habitable zone (HZ). Ocean planets that form outside the ice line and migrate inwards to the HZ and beyond were defined in detail by Selsis et al. (2007) in that broader sense and are now known to exist due to mean density measurements of a few transiting exoplanets (see, e.g., Gautier et al. 2012; Cochran et al. 2011; Gilliland et al. 2013).

Until recently, all known candidates for ocean planets (Borucki et al. 2013) were found orbiting very close to their stars. Such planets, e.g., Kepler-18*b*, -20*b*, -68*b*, are very hot due to the high stellar flux, which ensures a smooth transition from an interior water envelope to a steam atmosphere with no liquid surface ocean (Rogers & Seager 2010; Valencia et al. 2006). The discovery of many planetary systems with tightly packed inner planets by the *Kepler* mission has opened the prospect for obtaining mean densities of Earth-size planets in the HZ by transit-timing variations where radial velocity amplitudes are too small to measure (Lissauer et al. 2011). Given the very low mean densities measured so far among the majority of such planets, e.g., those found in Kepler-11 (Lissauer et al. 2013), Kepler-20 (Gautier et al. 2012), and Kepler-36 (Carter et al. 2012), we anticipate that the first HZ super-Earths of radius below 2 Earth radii ( $R_{\oplus}$ ) are more likely to be *water-rich* planets than rocky *silicate-rich* ones. The recent discovery of the multiple transiting system Kepler-62, with two planets in its HZ (Borucki et al. 2013), illustrates this point. We are motivated by the discovery of Kepler-62*e* and -62*f* to consider a more general approach of computing surface and atmospheric conditions on

water-planets in the HZ, which could also form in situ with a high water content (Raymond et al. 2007). Here we will refer to these planets as water-planets, given our assumption of theoretical interior models with pure water composition in an envelope surrounding a silicate- and metal-rich core, but no implicit assumption about liquid versus icy surface or the planet formation origin of the water. We focus on the interface between the mantle and the atmosphere with the view of computing observable spectra.

Water-planets of Earth to super-Earth sizes in the HZ fall into at least two types of interior geophysical properties in terms of the effect on their atmosphere. In the first type, hereafter Type1, the core–mantle boundary connects silicates with high-pressure phases of water (e.g., Ice VI, VII), i.e., the liquid ocean has an icy bottom. In contrast, in Type2, the liquid ocean has a rocky bottom, though no silicates emerge above the ocean at any time. The second type is essentially a rocky planet when viewed in terms of bulk composition. Both subtypes could possess a liquid ocean outer surface, a steam atmosphere, or a full cover of surface Ice I, depending on their orbit within the HZ and the magnitude of their greenhouse effect. Frozen water-planets should show a subsequent increase in the surface albedo value due to high reflective ice covering a frozen surface and will be most easily detected by direct imaging missions operating in the visible, while an IR imaging search will preferentially detect warm water-planets. Surface and atmospheric conditions on water-planets in the HZ have not been the subject of detailed studies. Thus far, work has focused on issues of evaporation (Kuchner 2003; Valencia et al. 2006; Murray-Clay et al. 2009) and boundary conditions to interior models (Valencia et al. 2007; Grasset et al. 2009; Fu et al. 2010; Rogers & Seager 2010).

In this Letter, we develop an initial model for water-planet atmospheres to allow assessment of their observables with future telescopes. This model will be based on many explicit and implicit assumptions using Earth as a template but taking into account anticipated differences in outgassing, geochemical cycling, global circulation, etc. to assess their observables with future telescopes. In this Letter, we describe a set of atmospheric models and their underlying assumptions in Section 2, how

<sup>3</sup> Super-Earth size is used here for planets with radii between  $1.25 R_{\oplus}$  and  $2.0 R_{\oplus}$ .

they could be applied to interpret Kepler-62*e* and -62*f* as water-planets in Sections 3 and 4, and conclude in Section 5 with discussion and conclusions.

## 2. ATMOSPHERIC MODELS FOR WATER-PLANETS: BASIC ASSUMPTIONS

Here we assume that the initial composition of icy planetesimals that assemble into water-planets is similar to that of comets: mostly H<sub>2</sub>O, and some NH<sub>3</sub>, and CO<sub>2</sub>. An initial composition of ice similar to that of comets leads to an atmospheric model composition of 90% H<sub>2</sub>O, 5% NH<sub>3</sub>, and 5% CO<sub>2</sub> (see also Leger et al. 2004, who simplified the atmospheric photochemistry by assuming no CO or CH<sub>4</sub>). NH<sub>3</sub> is UV sensitive, photodissociates, and is converted into N<sub>2</sub> and H<sub>2</sub> in a very short time frame, with H<sub>2</sub> being lost to space (see, e.g., Leger et al. 2004; Lammer et al. 2009). This shows that water-planet atmospheres should have the same chemical constituents as ocean land planets.

The carbonate–silicate cycle that regulates CO<sub>2</sub> on our own planet is effective due to the weathering of the exposed solid rock surface. Recent work (Abbot et al. 2012) has shown that, for an Earth-like planet, the carbonate–silicate cycle could continue to function largely unchanged for a continent surface fraction as low as 10%, with mid-ocean ridges taking over some of the recycling processes but argued that CO<sub>2</sub> cannot build up in the atmosphere of a Type2 water-planet without continents. Therefore, the HZ for water-planets was inferred to be narrower than for planets with continents.

Note that the arguments presented in that work are generally only applicable to Type2 water-planets, i.e., those with very low water-mass fraction. For Type1 water-planets, i.e., super-Earths with water-mass fractions like Earth ( $(2-5) \times 10^{-4}$ ) or above, the deep oceans are separated from the rocky interior via a layer of high-pressure ices. Therefore, an alternative mechanism to modulate abundant gases like CO<sub>2</sub> and CH<sub>4</sub> will be required in water-planets. Such a mechanism would depend on the properties of their clathration in water over a range of very high pressures. Methane clathrates are water molecule lattices that trap CH<sub>4</sub> molecules as guests by virtue of multiple hydrogen-bonding frameworks. Under very high pressures (above 0.6 GPa), common to super-Earth-size water-planets, methane clathrates undergo a phase transition in their structure to a form known as filled ice. Levi et al. (2013) studied this transition and concluded that CH<sub>4</sub> would be transported efficiently through the high-density water–ice mantle of water-planets in filled ice clathrates and eventually released in the atmosphere. It is well known that CO<sub>2</sub> substitutes CH<sub>4</sub> readily in normal-pressure clathrates (see, e.g., Park et al. 2006; Nago & Nieto 2011). We expect that this property can be extrapolated to filled ice, though this needs to be established. If so, this substitution will enable effective *cycling* of CO<sub>2</sub> through the atmosphere *and oceans* in water-planets residing in the HZ (e.g., with water oceans at the surface) and thus provide an atmospheric *concentration* feedback mechanism for CO<sub>2</sub> on water-planets. Abundant gases like CH<sub>4</sub> and CO<sub>2</sub> will be transported through the high-pressure phases of the planets mantle (filled ice and Structure I clathrates), through the liquid water ocean, then into the atmosphere, balanced by solubility in the ocean (depending on CO<sub>2</sub> solubility versus temperature), and the sequestration of CO<sub>2</sub> in clathrates. Similar to Earth-like planets with continents, such a cycle would control the CO<sub>2</sub> levels on water worlds, leading to water-dominated atmospheres for strong stellar irradiation and CO<sub>2</sub>-dominated atmosphere for low stellar irradiation.

This new water-planet model implies that atmospheric *composition* for water-planets in the HZ should not differ substantially from those of land-ocean planets, except for an increase in absorbed stellar flux due to the decreased surface reflectivity of water-planets (see Section 5).

## 3. THE HABITABLE ZONE FOR WATER-PLANETS

The “narrow” HZ is defined here classically as the annulus around a star where a rocky planet with a CO<sub>2</sub>/H<sub>2</sub>O/N<sub>2</sub> atmosphere and sufficiently large water content (such as on Earth) can host liquid water on its solid surface (Kasting et al. 1993; Abe et al. 2011; Pierrehumbert & Gaidos 2011). A conservative estimate of the range of the narrow HZ is derived from atmospheric models by assuming that the planets have a H<sub>2</sub>O- and CO<sub>2</sub>-dominated atmosphere with no cloud feedback on the edges of the HZ and determined based on the stellar flux intercepted by the planet (see Kopparapu et al. 2013 for details). Cloud feedback widens the limits of the HZ (see, e.g., Selsis et al. 2007; Zsom et al. 2012), but no consistent model yet exists, therefore we use the empirical value for the HZ from our own solar system as the “effective” HZ, defined by the initial solar fluxes received at the orbits of Venus (1 Gyr) and Mars (3.5 Gyr) when there was no liquid water on their surfaces. In this model, it is assumed that the planets are geologically active and that climatic stability is provided by a mechanism in which atmospheric CO<sub>2</sub> concentration varies inversely with planetary surface temperature.

The HZ changes only slightly for water-planets compared to land-ocean planets because at the limits of the HZ, the albedo is solely dominated by the atmosphere (see Figure 3 for insight on the effect of the surface albedo on the resulting atmospheric structure). Within the HZ for a given incident stellar flux, a water-planet has larger surface temperature due to the low surface reflection of water compared to land.

Cloud coverage influences the atmospheric temperature structure as well as the observability of spectral features (see, e.g., Kaltenecker et al. 2007; Kaltenecker & Traub 2009; Rauer et al. 2011.) On Earth cloud fractions are similar over water and land (see, e.g., Zsom et al. 2012). If sufficient cloud condensation nuclei are available, cloud coverage should be the same as for rocky planets for the same stellar insolation, but it will vary depending on the water-planet’s position in the HZ (Rugheimer et al. 2013, in preparation). The position and pattern of individual cloud layers depend on unknown planetary parameters like rotation rate. We mimic the effects of varying cloud coverage by varying the initial surface albedo in our atmospheric model from the standard value of 0.2 (used by Kasting et al. 1993; Kopparapu et al. 2013).

The atmospheric structure as well as the resulting HZ limits depend on the density of a planet’s atmosphere, shifting the HZ outward for lower mass and inward for higher mass planets (see also Kasting et al. 1993; Kopparapu et al. 2013). Without any further information on the relation of surface pressure to planetary mass, we make the first-order assumption here, that if outgassing rates per m<sup>2</sup> are held constant on a solid planet, and atmospheric loss rates decrease with planetary mass due to increased gravity, assuming a similar stellar environment, then a more massive planet should have a higher surface pressure (for similar outgassing and atmospheric loss mechanisms). In this Letter, we scale the surface pressure of the planet to first order with its surface gravity (following, e.g., Kaltenecker et al. 2011) and explore the effect of different planetary mass in Figure 3.

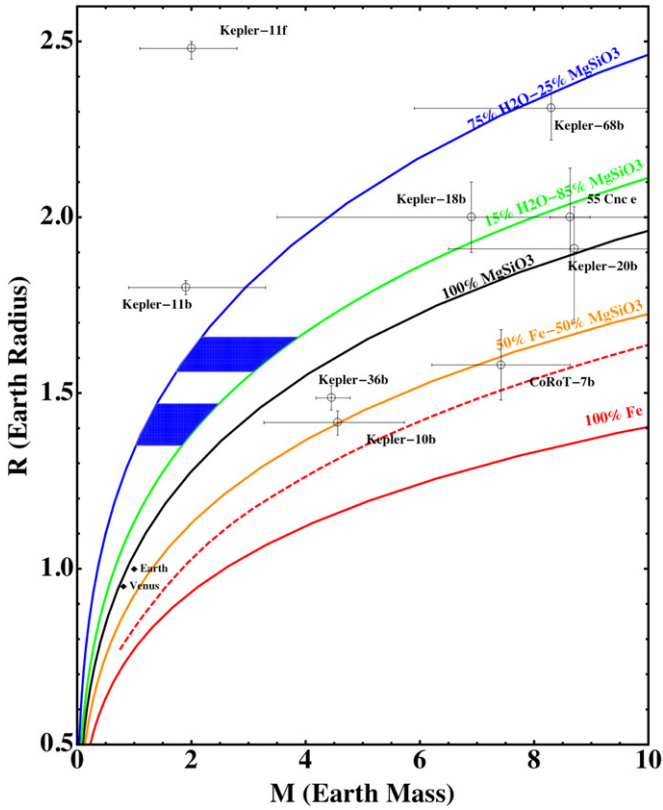


**Figure 1.** Mass–radius plot showing Kepler-62*e* and -62*f* as presumed water-planets (blue lozenges), compared to Venus, Earth, and transiting exoplanets. Kepler-69*c* ( $R_p = 1.7 (+0.34 - 0.23) R_E$ ) is not shown due to its very large error bars. The curves are theoretical models (Zeng & Sasselov 2013); the dashed line is the maximum mantle stripping limit (Marcus et al. 2010).

(A color version of this figure is available in the online journal.)

We use EXO-P (see, e.g., Kaltenegger & Sasselov 2010 for details and references) to model the atmosphere of water-planets. EXO-P consists of a coupled one-dimensional (1D) radiative–convective atmosphere code developed for rocky exoplanets based on a 1D-climate, 1D-photochemistry, and 1D-radiative transfer model.

#### 4. MODELS FOR TRANSITING TYPE I WATER-PLANETS IN THE HZ—THE KEPLER-62 AND -69 SYSTEMS

Kepler-62 (Borucki et al. 2013) and Kepler-69 (Barclay et al. 2013) are multi-transiting planet systems with individual planets in or close to the HZ (Figures 1 and 2). Kepler-62*e*, and -62*f* have radii of 1.61 and 1.41  $R_E$  with less than 5% errors, orbiting a K2V star of  $4925 \pm 70$  K ( $0.21 \pm 0.02 L_\odot$ ) at periods of 122.4 and 267.3 days, respectively (Borucki et al. 2013). They are super-Earth-size planets in the HZ of their host star, receiving  $1.2 \pm 0.2$  and  $0.41 \pm 0.05$  times the solar flux at Earth’s orbit ( $S_0$ ). Kepler-69*c* has a radii of  $1.7 (+0.34 - 0.29) R_E$  orbiting a  $5638 \pm 168$  K Sun-like star and semimajor axis to stellar radius ratio  $a/R_{\text{Star}} = 148 (+20 - 14)$  at periods of 242.5 days (Barclay et al. 2013). Due to the large uncertainty in luminosity of the star, Kepler-69*c* receives  $1.91 (+0.43 - 0.56) S_0$ .

The small radii of Kepler-62*e*, -62*f*, and -69*c* indicate that the planets should not have retained primordial hydrogen atmospheres at their insolation and estimated ages (Rogers & Seager 2010; Lopez et al. 2012; Lammer et al. 2009; Pierrehumbert & Gaidos 2011), making them strong candidates for solid planets and not mini-Neptunes. Given the large amount

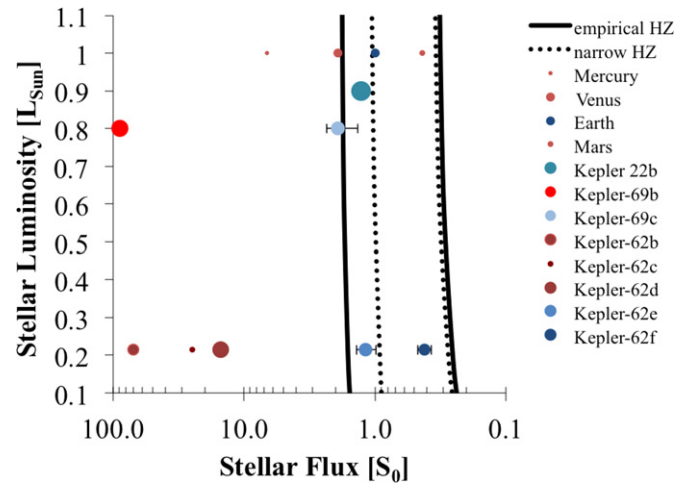


**Figure 2.** Comparison of known transiting exoplanets with measured radii less than  $2.5 R_\oplus$  in the HZ to the solar system planets. The sizes of the circles indicate the relative sizes of the planets to each other. The dashed and the solid lines indicate the edges of the narrow and effective HZ, respectively.

(A color version of this figure is available in the online journal.)

of solid objects already present in the Kepler-62 system on orbits inward of -62*e*, and following the recent results on the Kepler-11 cohort of six low-density planets with tightly packed close-in orbits (Lissauer et al. 2013), it strongly suggests that -62*e* and -62*f* formed outside the ice line and are therefore our first HZ water-planets. While other possibilities remain open until their actual masses are measured, for the purposes of this Letter we assume that they are indeed water-planets on low-eccentricity orbits and model both biotic and abiotic atmospheres.

For Kepler-62*e*, we set the  $O_2$  mixing ratio to 0.21 (biotic),  $0.21 \times 10^{-6}$  (abiotic). We set  $CO_2$  to 10 ppm for Kepler-62*e* at the inner part of the HZ, which corresponds to the conservative lower limit for C4 photosynthesis (Heath 1969; Pearcy & Ehleringer 1984). For Kepler-62*f*, we calculate  $CO_2$  levels necessary to maintain liquid water on its surface, which results in 5 bar of  $CO_2$  for the considered albedo range. For Kepler-62*f*, we set  $O_2$  to 0.21 atm for the biotic model because maintaining a constant mixing ratio of 0.21 would yield unrealistically high  $O_2$  pressures (about 1 bar). The  $CH_4$  flux is set to  $1.31 \times 10^{11}$  (biotic; Rugheimer et al. 2013) and  $4 \times 10^{-9}$  molecules  $cm^{-2} s^{-1}$  (abiotic; see e.g., Kasting & Catling 2003; Segura et al. 2005) for both planets.

#### 5. DISCUSSION AND CONCLUSIONS

For Kepler-62*e*’s radius, a water-planet’s mass would be in the range  $2-4 M_E$ . Kepler-62*f* has a smaller radius of  $1.41 R_E$ , so its mass would be  $1.1-2.6 M_E$ . The transition from liquid water to the first solid phase of Ice VI occurs at 0.63–2.2 GPa, depending on the temperature. Beyond 2.2 GPa, the solid phase water is Ice VII. The depth of the liquid ocean is thus in the range of 80–150 km for these two planets. The radius of Kepler-69*c*  $R_p = 1.7 (+0.34 - 0.23) R_E$  has very large error bars, therefore the mass range is ill-defined.

Figure 2 shows that the stellar flux values at the limit of the HZ are  $1.66-0.27 S_0$  for the effective HZ and  $0.95-0.29 S_0$  for the narrow HZ, respectively, for Kepler-62. The limits are  $1.78-0.29 S_0$  for the effective HZ and  $1.01-0.35 S_0$  for the narrow HZ for Kepler-69 (based on models by Kopparapu et al. 2013). The intercepted flux at the orbit of Kepler-62*e*

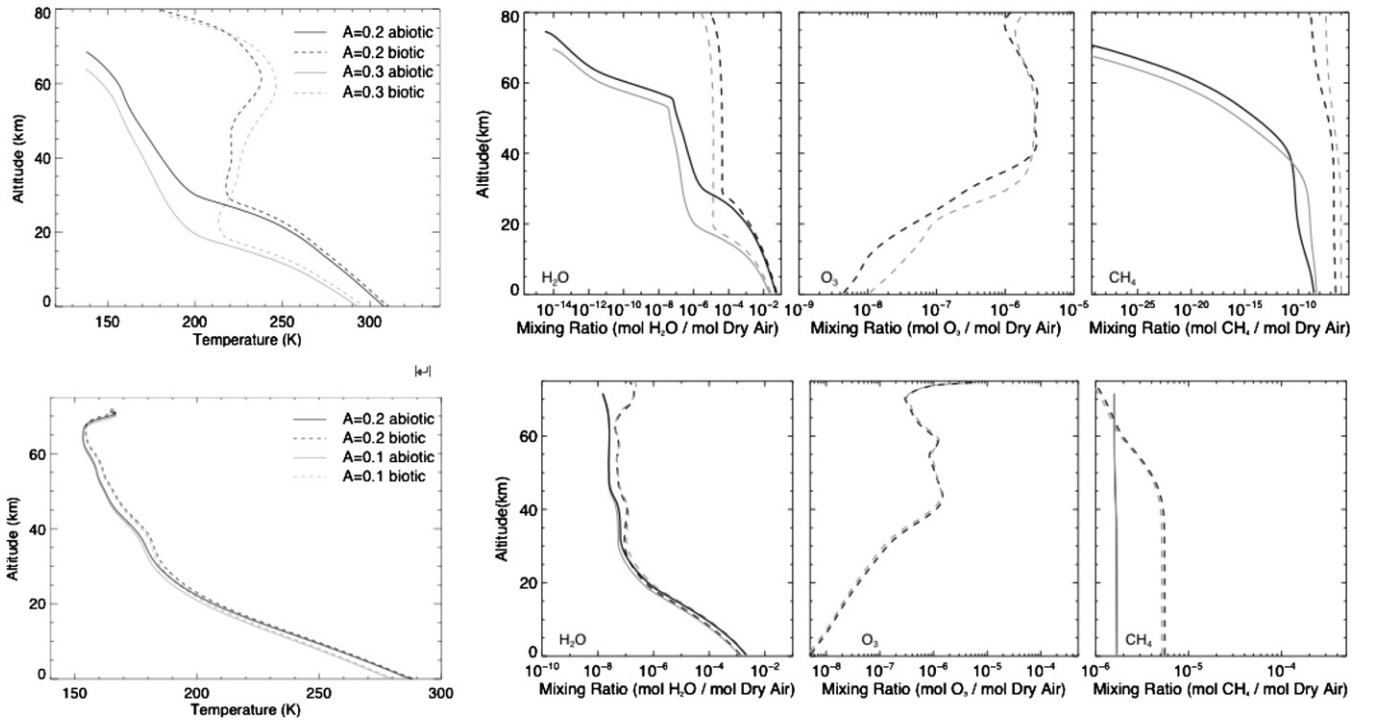


**Figure 3.** Temperature and mixing ratios for  $\text{H}_2\text{O}$ ,  $\text{O}_3$ , and  $\text{CH}_4$  for biotic and abiotic atmospheric models for water-planets in the inner (top) and outer (bottom) part of the HZ (using planetary parameters for Kepler-62e and -62f) for the smallest mass models.

and -62f makes both planets candidates for liquid water on their surface. If the atmosphere of Kepler-62f accumulates several bars of atmospheric  $\text{CO}_2$  (1.6–5 bar, depending on the model planetary mass and surface albedo) it could be covered by liquid water on its surface, otherwise it would be ice-covered. This first possibility allows for a warm Type1 water-planet in the inner and outer part of the HZ (Figure 4). The second possibility allows comparing a warm and cold Type1 water-planet in this system. These differences are similar to the variations with temperatures of rocky planet spectra, but water-planets are hotter at a given distance from their star.

Figure 2 shows that Kepler-69c lies outside the effective HZ when using the nominal stellar flux, but the error bar on the star’s flux allows for the possibility that the planet is within the empirical HZ.

To explore the atmospheric features of transiting water-planet, we concentrate on the Kepler-62 system here, where both planets are within the star’s HZ. We run Exo-P models tuned to the Kepler-62 parameters. We also explore the effect of changing cloud parameters by varying the surface albedo from 0.2 to 0.3 mimicking increased water cloud coverage for Kepler-62e, and from 0.2 to 0.1 for Kepler-62f mimicking decreased water cloud coverage. Figure 3 shows the atmospheric structure of both planets as Type1 water-planets for the minimum mass and explore their changes with surface albedo (nominally 0.2). Interior models (see Zeng & Sasselov 2013) of Kepler-62e models give a scaled surface pressure of 0.78–1.56 times Earth’s and surface temperatures for the low-mass case of ( $A = 0.2$ ) 303 K and 306 K and ( $A = 0.3$ ) 292 K and 296 K for the abiotic and biotic cases, respectively. Models for the high planetary mass case result in surface temperatures of ( $A = 0.2$ ) 307 K and 310 K and ( $A = 0.3$ ) 293 K and 297 K for the abiotic and biotic cases, respectively, showing a slightly higher surface temperature for planets with higher mass and surface pressure.

Atmospheric models for Kepler-62f show that 1.6 bar ( $A = 0.1$ ) and 5 bar ( $A = 0.3$ ) of  $\text{CO}_2$  are needed to warm the surface temperature above freezing. Models of Kepler-62f lead to a scaled surface pressure of 0.56–1.32 times Earth’s. We add 5 bar of  $\text{CO}_2$  to this pressure, which results in surface temperatures of 288 K and 289 K ( $A = 0.1$ ) and 280 K and 281 K ( $A = 0.2$ ) for the abiotic and biotic cases, respectively. For the high-mass case of Kepler-62f, we obtain surface temperatures of 297 K and 298 K ( $A = 0.1$ ) and 285 K and 287 K ( $A = 0.2$ ) for the abiotic and biotic cases, respectively.

Figure 4 uses two model calculations (the lowest surface pressure and gravity consistent with Kepler-62e and -62f, for biotic conditions) to generate transmission spectra that can inform future instrument sensitivity requirements. This choice allows us to model the maximum observable spectral features among the models, due to the low gravity. Using the highest planetary mass in the interior models would decrease the observable spectral features by a factor of about two.

Figure 4 shows the corresponding synthetic transmission spectra of (top) a water-dominated atmosphere warm water-planet (using model parameters for a light Kepler-62e) and (middle) a  $\text{CO}_2$ -dominated atmosphere frozen water-planet (using model parameters for a light Kepler-62f with only 100PAL  $\text{CO}_2$ ), and of a current Earth analog (bottom). The comparison clearly shows stronger  $\text{CO}_2$  in the transmission spectra of a water-planet on outer edge of the HZ compared to a water-planet the inner edge of the HZ. Therefore, relatively low resolution spectra allow such planets to be characterized for telescopes like *James Webb Space Telescope* (see, e.g., Kaltenegger & Traub 2009; Deming et al. 2009; Rauer et al. 2011; Belu et al. 2011; von Paris et al. 2013) as well as high-resolution ground-based telescopes like European Extremely Large Telescope (Snellen et al. 2013).

We have defined two types of water-planets, Type1, which are true water-planets in their bulk composition, and Type2,

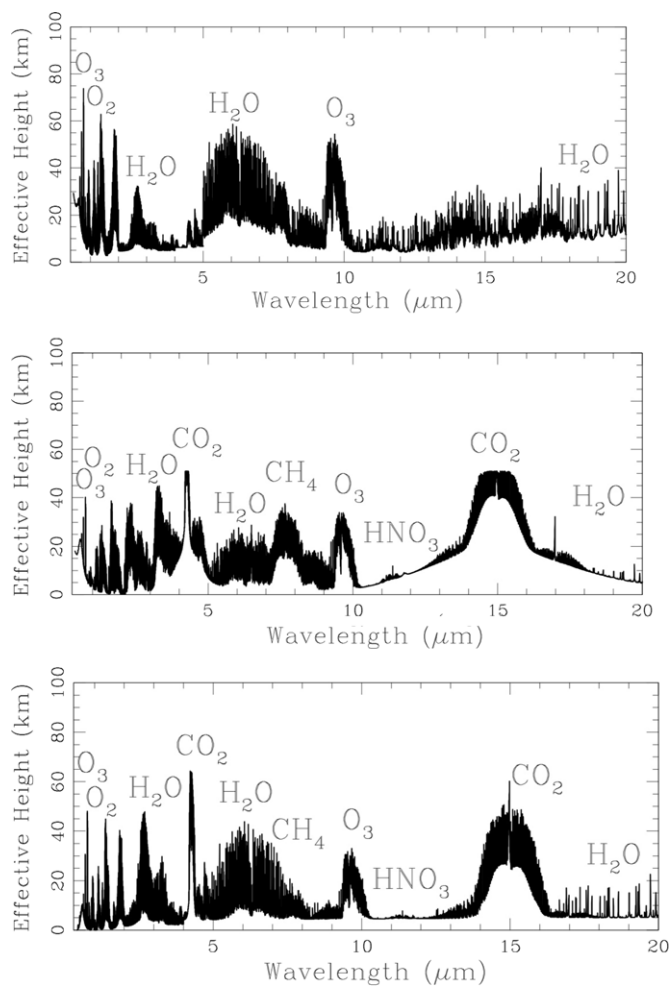


**Figure 4.** Synthetic transmission spectra of atmospheric models for a hot (top) and cold (middle) water-planet, using Kepler-62*e* and -62*f* parameters for the smallest mass models (see the text), and the Earth in transit (bottom) for comparison.

which are rocky planets with water covering all surface and postulated a new cycling mechanism for CO<sub>2</sub> using clathrates. A detailed atmospheric model of the specific planets of Kepler-62*e* and -62*f* as Type 1 water-planets permits for liquid water on each, if -62*f* accumulates several bar of CO<sub>2</sub> in its atmosphere. We introduce a potential CO<sub>2</sub> cycling mechanism on water-planets. The Kepler-62*e* models show a warm water-planet between the limits of the narrow HZ and the effective HZ. Figure 4 shows that the transmission spectrum of a water-planet allows an interesting comparison of warm water- versus CO<sub>2</sub>-dominated as well as warm and cold water-planets in this system. These differences are similar to the variations with temperatures of rocky planet spectra, but water-planets are *slightly* hotter at a given distance from their star.

Kepler-62*e* and -62*f* are the first viable candidates for HZ water-planets which would be composed of mostly solids, consisting of mostly ice (due to the high internal pressure) surrounding a silicate-iron core. The nominal flux intercepted

at Kepler-62*c* is too high for it to be in the effective HZ, but the large error bars on its star's flux allow for this planet close to the inner edge of the empirical HZ.

Water-planets in the HZ are completely novel objects that do not exist in our own solar system. The atmospheric models presented here predict detectable features in the spectra of water-planets in the HZ in transit. Therefore, we expect that future remote characterization will allow us to distinguish water-planets at different parts of their HZ.

The authors thank J. McDowell for in depth discussions. L. K. acknowledges support from DFG funding ENP Ka 3142/1-1, D. S. partial support by NASA NNX09AJ50A (Kepler Mission science team).

## REFERENCES

- Abbot, D. S., Cowan, N. B., & Ciesla, F. J. 2012, *ApJ*, **756**, 178  
 Abe, Y., Abe-Ouchi, A., Sleep, N. H., & Zahnle, K. J. 2011, *AsBio*, **11**, 443  
 Barclay, T., Burke, C. J., Howell, S. B., et al. 2013, *ApJ*, **768**, 101  
 Belu, A. R., Selsis, F., Morales, J., et al. 2011, *A&A*, **525**, A83  
 Borucki, W. J., Agol, E., Fressin, F., et al. 2013, *Sci.*, **340**, 587  
 Carter, J. A., Agol, E., Chaplin, W. J., et al. 2012, *Sci.*, **337**, 556  
 Cochran, W. D., Fabrycky, D. C., Torres, G., et al. 2011, *ApJS*, **197**, 7  
 Deming, D., Seager, S., Winn, J., et al. 2009, *PASP*, **121**, 952  
 Fu, R., O'Connell, R. J., & Sasselov, D. D. 2010, *ApJ*, **708**, 1326  
 Gautier, T. N., III, Charbonneau, D., Rowe, J. F., et al. 2012, *ApJ*, **749**, 19  
 Gilliland, R. L., Marcy, G. W., Rowe, J. F., et al. 2013, *ApJ*, **766**, 40  
 Grasset, O., Schneider, J., & Sotin, C. 2009, *ApJ*, **693**, 722  
 Heath, O. V. S. 1969, *The Physiological Aspects of Photosynthesis* (Redwood City, CA: Stanford Univ. Press)  
 Kaltenegger, L., & Sasselov, D. D. 2010, *ApJ*, **708**, 1162  
 Kaltenegger, L., Segura, A., & Mohanty, S. 2011, *ApJ*, **733**, 35  
 Kaltenegger, L., & Traub, W. A. 2009, *ApJ*, **698**, 519  
 Kaltenegger, L., Traub, W. A., & Jucks, K. W. 2007, *ApJ*, **658**, 598  
 Kasting, J. F., Whitmire, D. P., & Reynolds, R. T. 1993, *Icar*, **101**, 108  
 Kasting, J. F., & Catling, D. 2003, *ARA&A*, **41**, 429  
 Kopparapu, R., Ramirez, R., Kasting, J. F., et al. 2013, *ApJ*, **765**, 131  
 Kuchner, M. 2003, *ApJ*, **596**, L105  
 Lammer, H., Kasting, J. F., Chassefière, E., et al. 2009, *SSRv*, **139**, 399  
 Leger, A., Selsis, F., Sotin, C., et al. 2004, *Icar*, **169**, 499  
 Levi, A., Sasselov, D. D., & Podolak, M. 2013, *ApJ*, **769**, 29  
 Lissauer, J. J., Fabrycky, D. C., Ford, E. B., et al. 2011, *Nat*, **470**, 53  
 Lissauer, J. J., Jontof-Hutter, D., Rowe, J. F., et al. 2013, *ApJL*, **770**, L131  
 Lopez, E. D., Fortney, J. J., & Miller, N. K. 2012, *ApJ*, **761**, 59  
 Marcus, R., Sasselov, D. D., Hernquist, L., & Stewart, S. 2010, *ApJ*, **712**, L73  
 Murray-Clay, R. A., Chiang, E. I., & Murray, N. 2009, *ApJ*, **693**, 23  
 Nago, A., & Nieto, A. 2011, *JGR*, **2011**, 239397  
 Percy, R. W., & Ehleringer, J. 1984, *Plant Cell Envir.*, **7**, 1  
 Pierrehumbert, R., & Gaidos, E. 2011, *ApJL*, **734**, L13  
 Rauer, H., Gebauer, S., Paris, P. V., et al. 2011, *A&A*, **529**, A8  
 Raymond, S. N., Quinn, T., & Lunine, J. I. 2007, *AsBio*, **7**, 66  
 Rogers, L., & Seager, S. 2010, *ApJ*, **716**, 1208  
 Rugheimer, S., Kaltenegger, L., Zsom, A., et al. 2013, *AsBio*, **133**, 251  
 Segura, A., Kasting, J. F., Meadows, V., et al. 2005, *AsBio*, **5**, 706  
 Selsis, F., Kasting, J. F., Levrard, B., et al. 2007, *A&A*, **476**, 1373  
 Snellen, I. A. G., de Kok, R. J., le Poole, R., Brogi, M., & Birkby, J. 2013, *ApJ*, **764**, 182  
 Valencia, D., O'Connell, R. J., & Sasselov, D. D. 2006, *Icar*, **181**, 545  
 Valencia, D., O'Connell, R. J., & Sasselov, D. D. 2007, *ApJ*, **665**, 1413  
 von Paris, P., Hedelt, P., Selsis, F., Schreier, F., & Trautmann, T. 2013, *A&A*, **551**, A120  
 Park, Y., Kim, D.-Y., Lee, J.-W., et al. 2006, *PNAS*, **103**, 12690  
 Zeng, L., & Sasselov, D. 2013, *PASP*, **125**, 227  
 Zsom, A., Kaltenegger, L., & Goldblatt, C. 2012, *Icar*, **221**, 603